
A generic and expected long title added as a placeholder for actual long titles



Ohana Benevides Rodrigues

DEPARTMENT OF PHYSICS
COLLEGE OF ARTS AND SCIENCES
SYRACUSE UNIVERSITY

Dissertation presented as a partial fulfillment of the requirements for the degree of

Doctor of Philosophy in Physics

SYRACUSE - NY

2022

Substitua essa folha pela FOLHA DE APROVAÇÃO ou ATA DA DEFESA.

*To my parents, Andrea de Fátima Benevides and
Luis Claudio Rocha Rodrigues.*

Acknowledgements

The acknowledgements.

“Knowledge emerges only through invention and reinvention, through the restless, impatient, continuing, hopeful inquiry human beings pursue in the world, with the world, and with each other.”

Paulo Freire

Contents

Acknowledgements	ix
1 Introduction	1
1.1 Neutrino Physics Historical Overview	1
1.1.1 The Beta Decay Problem	1
1.1.2 The First Neutrino Measurement	1
1.2 Different Types of Neutrinos	2
1.2.1 The Solar Neutrinos Flux Problem	3
1.2.2 Neutrino Oscillation	4
1.2.3 Current Neutrino Oscillation Model	5
1.3 Current Understanding of Neutrino Physics	7
1.4 LArTPCs in Neutrino Physics	12
1.5 The Short Baseline Neutrino Program	13
1.6 The Deep Underground Neutrino Experiment	14
2 μ Decay At Rest ν_e-LAr CC Cross Section in MicroBooNE	17
2.1 Core-Collapse Supernova Neutrino Detection in DUNE	17
2.2 μ Decay At Rest (μ DAR)-LAr Physics	17
2.3 MicroBooNE	17
2.4 NuMI	17
2.5 Simulation of μ DAR Events in MicroBooNE	17
2.5.1 NuMI Beamline Simulation	17
2.5.2 GENIE and MARLEY	17
2.6 Reconstruction of μ DAR Events in MicroBooNE	17
2.7 Monte Carlo-Data Agreement	17
2.8 Background Assessment	17
2.9 Data Analysis	17
2.10 Conclusion	17

3 Short Baseline Neutrino Detector's (SBND) Anode Plane Assemblies (APA) Assembly and Installation	19
3.1 APA Description	19
3.2 APA Quality Assurance (QA) and Quality Control (QC) Tests	19
3.3 APA Installation Procedures	19
3.4 Status	19
4 Novel LAr Purity Monitor Using Paul Traps	21
4.1 Purity Monitors for LArTPCs	21
4.1.1 Motivation	21
4.1.2 Current Methods	21
4.2 Paul Trap as a Purity Monitor	21
4.2.1 Concept and Design	21
4.2.2 Simulation	21
4.3 Conclusion and Next Steps	21
A An appendix title	23

List of Figures

1.1	The beta decay spectrum of tritium	2
1.2	Three Flavor Oscillation Model	7
1.3	Inside Super-Kamiokande tank	8
1.4	Feymann Diagrams for the two types of weak interactions	9
1.5	Total CC neutrino cross-section per nucleon as function of energy	9
1.6	The Mass Hierarchy	10
1.7	Preliminary θ_{23} results from the NO ν A Experiment	11
1.8	LArTPC	12
1.9	LArTPC read out system	13
1.10	SBN Program	14
1.11	DUNE’s full schematic	15

List of Tables

1.1	The lepton family	3
-----	-----------------------------	---

1

1

2

3
4

Introduction

5 1.1 Neutrino Physics Historical Overview

6 1.1.1 The Beta Decay Problem

Radioactivity was discovered in 1896 by Henri Becquerel. A few years later, in 1899, Ernest Rutherford classified radioactivity emissions into two types: α and β . In the occasion, Rutherford conjectured that the beta decay was a two-body decay. In such case, the decay would be characterized by a nucleus A becoming a lighter nucleus B, with the emission of an electron, like the following:

$$A \longrightarrow B + e^-.$$
 (1.1)

Consequently, the energies of the outgoing particles would be kinematically determined. Using conservation of energy and momentum, it is straightforward to conclude that this energy should be:

$$E = \frac{m_A^2 - m_B^2 + m_e^2}{2m_A} c^2.$$
 (1.2)

7 Experiments conducted by Lise Meitner and Otto Han in 1911 demonstrated that the energy
8 spectrum of the electron coming out of the β decay was, in fact, not well-defined, as expected
9 if it was two-body decay. The electron energy spectrum was continuous, having the maximum
10 energy defined by the equation 1.2 (see figure 1.1) [1].

11 In 1930, Wolfgang Pauli proposed that the beta decay was not a two-body decay, but a
12 three-body decay. He predicted that the third particle proposed by him would be neutral and
13 light. Pauli originally named it neutron. Later, with Chadwick's discovery of the neutron, Fermi
14 changed the name of his predicted particle to neutrino [1]. A few years later, in 1933, Pauli and
15 Perrin proposed that neutrinos were massless [1].

16 1.1.2 The First Neutrino Measurement

It was not until 1956 that neutrinos were experimentally verified by Cowan and Reines. They conducted an experiment at the Savannah River nuclear reactor in South Carolina that

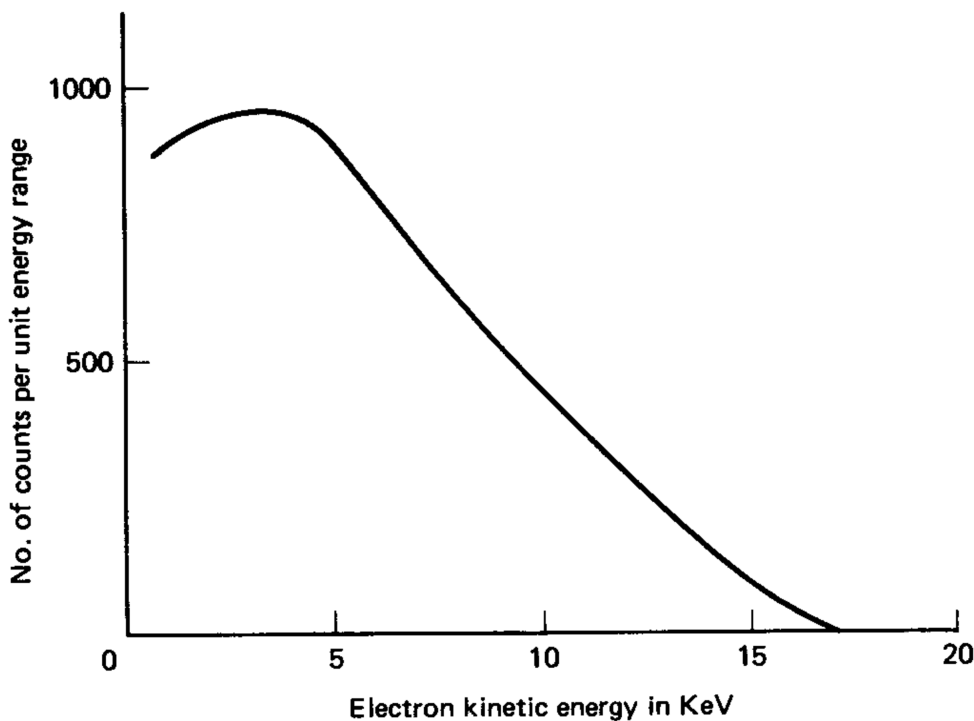
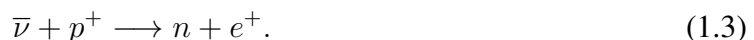


Figure 1.1 | The beta decay spectrum of tritium

The figure shows the electron energy spectrum in a beta decay of tritium [1].

consisted of a big tank of water and cadmium chloride, surrounded by 4,200 liters of liquid scintillator, seated near the nuclear reactor. If neutrinos, as predicted by Pauli, were real, they would be produced by the nuclear reaction inside the reactor and, as entering the detector, would possibly hit the protons of the water and produce a positron and a neutron. This reaction is called inverse beta decay, and it is given as:



¹⁷ The reaction's signature they were looking for were two photons, produced by the electron-
¹⁸ positron annihilation, and, a few microseconds later, a few photons, produced by the neutron
¹⁹ capture by the cadmium [2]. They published their results in a paper called “Detection of the
²⁰ Free Neutrino: A Confirmation”, confirming the existence of neutrinos (Ref. [3]).

²¹ 1.2 Different Types of Neutrinos

²² In 1953, Konopinski and Mahmoud proposed the existence of a lepton number and the con-
²³ versation of it, which could explain why certain reactions happen and some others do not. As
²⁴ convention, it was established that leptons would have a lepton number $L = 1$, that antileptons
²⁵ would have lepton number $L = -1$, and that any other particle would have lepton number $L =$
²⁶ 0. By this rule, an antineutrino should be produced in a beta decay. Although the rule explained

	Lepton number	Electron number	Muon number
Leptons			
e^-	1	1	0
ν_e	1	1	0
μ^-	1	0	1
ν_μ	1	0	1
Antileptons			
e^+	-1	-1	0
$\bar{\nu}_e$	-1	-1	0
μ^-	-1	0	-1
ν_μ	-1	0	-1

Table 1.1 | The lepton family from 1962 to 1976 [1]

²⁷ why many reactions supposedly allowed to happen were not observed, it still did not explain a
²⁸ few cases. This led them to postulate the existence of a lepton number for each of the leptons.
²⁹ That is, a muon number, an electron number and, years later, a tau number (see table 1.1) [4].

³⁰

³¹ This hypothesis was experimentally checked in 1962 at the Brookhaven National Laboratory
³² by Lederman, Schwartz e Steinberger. Their experiment consisted of having a beam of charged
³³ pions, produced in a particle accelerator called Alternating Gradient Synchrotron (AGS), and
³⁴ observing the neutrinos that accompanied the muons produced whenever the beam pions de-
³⁵ cayed. Hypothetically, if the lepton number is the same for muons and electrons, the following
³⁶ reactions are allowed and, consequently, should be observed:

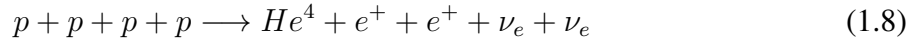


³⁸ action of neutrinos produced with a muon can only produce other muons. That is, each lepton
³⁷ In the experiment only the third and fourth reactions were observed, implying that the inter-
³⁹ has a corresponding neutrino [5].

⁴⁰ 1.2.1 The Solar Neutrinos Flux Problem

The series of nuclear reactions occurring in the solar and stellar cores are given by the so-called carbon–nitrogen–oxygen (CNO) cycle and the pp-chain. In the CNO cycle the four

protons are successively absorbed in a series of nuclei, starting and ending with carbon. In the pp-chain two protons combine to form the deuteron and further protons are added [6]. In either case, the net process is:



Ray Davis proposed an experiment to measure the neutrinos emitted by the sun. The experiment was based on the following inverse beta decay.



41 The main idea was that the chlorine would absorb a solar neutrino and would produce an elec-
42 tron and an Ar³⁷. A tank containing 615 tons of a fluid rich in chlorine called tetrachloroethylene
43 was placed in the Homestake gold mine in South Dakota. The fluid was periodically purged with
44 Helium gas to remove the argon-37 atoms, which were then counted by means of their radioac-
45 tivity. In the average, the experiment measured one neutrino after every three days and ran for
46 30 years. Although the measurement of solar neutrinos was a success, the experiment measured
47 a flux 2/3 smaller than the one theoretically predicted by John Bahcall. This difference became
48 known as the solar neutrino problem and the results were published in 1970 [6].

49 1.2.2 Neutrino Oscillation

50 In 1967 Bruno Pontecorvo published a paper called “Neutrino Experiments and The Prob-
51 lem of Conservation of Leptonic Charge” in which he discussed the effect of neutrino oscilla-
52 tions for the solar neutrinos. He wrote [7]:

53 “From an observational point of view the ideal object is the sun. If the oscillation
54 length is smaller than the radius of the sun region effectively producing neutrinos,
55 direct oscillations will be smeared out and unobservable. The only effect on the
56 earth’s surface would be that the flux of observable sun neutrinos must be two
57 times smaller than the total (active and sterile) neutrino flux.”

58 Thus, Pontecorvo anticipated the solar neutrino problem!

59 The next paper about neutrino oscillations was published two years later by V. Gribov and B.
60 Pontecorvo. They considered a scheme of neutrino mixing and oscillations with four neutrino
61 and antineutrino states: two left-handed states of neutrinos, ν_e and ν_μ , and two right-handed
62 states of antineutrinos, $\bar{\nu}_e$ and $\bar{\nu}_\mu$. The main assumption of Gribov and Pontecorvo was that
63 there are no sterile neutrino states [8].

64 1.2.3 Current Neutrino Oscillation Model

65 The current model of oscillations considers three neutrinos: The electron neutrino, the muon
66 neutrino and the tau¹

In this model, a neutrino flavor eigenstate with momentum \vec{p} can be written as a linear combination of the neutrino mass eigenstates:

$$|\nu_\alpha\rangle = \sum_{k=1}^n U_{\alpha k}^* |\nu_k\rangle, \quad (1.10)$$

Where $\alpha = e, \mu, \tau$; $|\nu_k\rangle$ is the mass base, k is the known mass states and U is the Pontecorvo-Maki-Nakagawa-Sakata (PMNS) matrix [10, 11], that is:

$$U = \begin{pmatrix} 1 & 0 & 0 \\ 0 & c_{23} & s_{23} \\ 0 & -s_{23} & c_{23} \end{pmatrix} \begin{pmatrix} c_{13} & 0 & s_{13}e^{-i\delta} \\ 0 & 1 & 0 \\ -s_{13}e^{+i\delta} & 0 & c_{13} \end{pmatrix} \begin{pmatrix} c_{12} & s_{12} & 0 \\ -s_{12} & c_{12} & 0 \\ 0 & 0 & 1 \end{pmatrix} \quad (1.11)$$

67 where $c_{ij} \equiv \cos(\theta_{ij})$, $s_{ij} \equiv \sin(\theta_{ij})$ and δ is the Charge Parity (CP) symmetry violating
68 phase parameter. In equation 1.11, the three matrices represent different neutrino oscillation
69 sectors. The left matrix represents the accelerator neutrino sector, the middle matrix represents
70 the transition $\nu_e \rightarrow \nu_\tau$, that is present in both accelerator and reactor neutrino sectors, and the
71 right matrix represents the reactor neutrino sector.

Consider that the flavor eigenstates are orthogonal, that the mass eigenstates are also orthogonal, that the PMNS matrix is unitary, that the neutrinos are oscillating in the vacuum, and also that the mass eigenstates are hamiltonian's eigenstates. The last statement leads to:

$$H|\nu_k\rangle = E_k|\nu_k\rangle \quad (1.12)$$

That means that the energy eigenvalues are

$$E_k = \sqrt{\vec{p}^2 + m_k^2}. \quad (1.13)$$

If we evolve the mass eigenstate in time, it is possible to write the flavor eigenstate as

$$|\nu_\alpha(t)\rangle = \sum_{k=1}^n U_{\alpha k}^* e^{-iE_k t} |\nu_k\rangle. \quad (1.14)$$

¹The tau neutrino particle was detected in 1997 by The Direct Observation of NU Tau (DONuT) experiment at Fermi National Laboratory (Fermilab) [9].

Rewriting equation 1.14 only in the flavor base yields

$$|\nu_\alpha(t)\rangle = \sum_{\beta=e,\mu,\tau} \left(\sum_{k=1}^n U_{\alpha k}^* U_{\beta k} e^{-iE_k t} \right) |\nu_\beta\rangle. \quad (1.15)$$

The term between parenthesis is the $\nu_\alpha \rightarrow \nu_\beta$ transition amplitude. With that information and some more algebra it is possible to show that the time dependent transition probability is

$$P_{\nu_\alpha \rightarrow \nu_\beta}(t) = \sum_{k=1}^n \sum_{j=1}^n U_{\alpha k}^* U_{\beta k} U_{\alpha j} U_{\beta j}^* e^{i(E_k - E_j)t}. \quad (1.16)$$

Some approximations and simplifications are possible. As neutrino masses are extremely small, they are in a relativistic regime. This allow the approximation, through Taylor expansion

$$E_k - E_j \approx \frac{m_k^2 - m_j^2}{2E} = \frac{\Delta m_{kj}^2}{2E}. \quad (1.17)$$

As neutrino's velocity is close to the light's one in vaccum

$$L \approx ct = t. \quad (1.18)$$

⁷² Separating the exponential in the equation 1.16 into real and imaginary parts, the indexes in
⁷³ $k = j$ and $k > j$, and using some more algebra the final result is

$$\begin{aligned} P_{\nu_\alpha \rightarrow \nu_\beta}(L/E) &= \delta_{\alpha\beta} - 4 \sum_{k>j}^n \Re[U_{\alpha k}^* U_{\beta k} U_{\alpha j} U_{\beta j}^*] \sin^2 \left(\frac{\Delta m_{kj}^2 L}{4E} \right) \\ &\quad + 2 \sum_{k>j}^n \Im[U_{\alpha k}^* U_{\beta k} U_{\alpha j} U_{\beta j}^*] \sin \left(\frac{\Delta m_{kj}^2 L}{2E} \right). \end{aligned} \quad (1.19)$$

⁷⁴ In figure 1.2, you will find a plot for the three flavor oscillation probabilities as a function
⁷⁵ of L/E_ν , assuming the original state is ν_μ

⁷⁶ For the antineutrinos, the mathematical steps are similar from the ones we just took [12].

⁷⁷ First Neutrino Oscillation Measurements

⁷⁸ The first oscillation measurements, and consequently the confirmation that neutrinos have
⁷⁹ mass, were made by the Super-Kamiokande experiment. The Super-Kamiokande detector is lo-
⁸⁰ cated 1 km underground in the Kamioka-mine, Hida-city, Gifu, Japan. It consists of a stainless-
⁸¹ steel tank, with 39.3 m of diameter and 41.4 m tall, filled with 50,000 tons of ultra pure water.
⁸² It has about of 13,000 photo-multipliers installed on the tank's wall (see image 1.3). In 1998
⁸³ the Super-Kamiokande collaboration published the first neutrino oscillation measurements in a
⁸⁴ paper called "Evidence for oscillation of atmospheric neutrinos" [14].

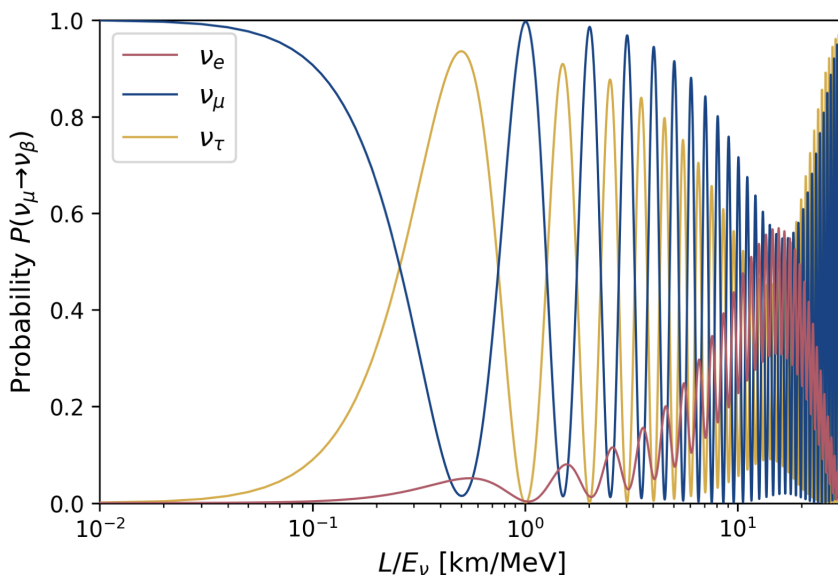


Figure 1.2 | Three Flavor Oscillation Probabilities as a Function of L/E_ν Three Flavor Oscillation Probabilities as a Function of L/E_ν , assuming the original state is ν_μ , [13].

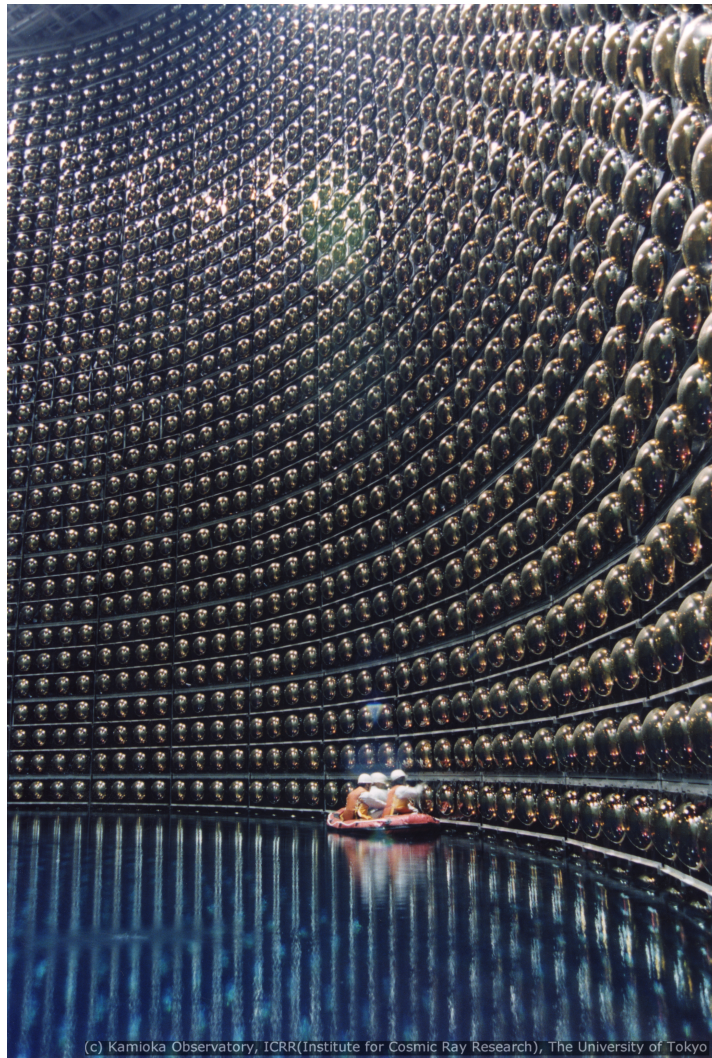
85 1.3 Current Understanding of Neutrino Physics

86 At this point, allow me to briefly summarize the understanding we currently have of neutrinos, obtained through the experiments and studies I mentioned above and also by many other 87 experiments I left out from this historical overview.

88 Neutrinos are chargeless leptons with small non-zero mass that only interact through the weak force. So far, we know of the existence of three types of them, that we call "flavor", 89 and that are named after the charged lepton that accompanies them in charged-current weak 90 interactions: electron neutrino (ν_e), muon neutrino (ν_μ), and tau neutrino (ν_τ).

91 The weak interaction is mediated by three bosons: The Z^0 boson, responsible for carrying 92 the Neutral Current (NC) interactions, and the W^- and W^+ bosons, responsible for carrying the 93 Charged Current (CC) interactions. The Feynman Diagrams below represent said interactions. 94 In the CC neutrino interactions, we have an incoming neutrino interacting with a nucleus' quark 95 and producing a charged lepton, their neutrino counterpart, and a different nucleus' quark, such 96 as to conserve charge number. In the NC the incoming and outgoing particle natures remain the 97 same, but transfer momentum and energy.

98 We can observe different outcome final products from neutrino interactions, depending on 99 the energy of the incoming neutrino. At lower energies, $\lesssim 10$ GeV, the dominant processes 100 will be quasi-elastic scattering (QE), where neutrinos scatter off of a nucleon, and resonance, 101 where neutrinos scatter off of a nucleon that gets excited and decays. From 10 GeV beyond, 102 the dominant process is Deep Inelastic Scattering (DIS) where neutrinos scatter directly off 103 of nucleus' quarks. In figure 1.5 you can see a summary of the existing measurements of CC 104 105



(c) Kamioka Observatory, ICRR (Institute for Cosmic Ray Research), The University of Tokyo

Figure 1.3 | Inside Super-Kamiokande tank

Workers doing photomultipliers (PMTs) checking inside Super-Kamiokande detector [15].

¹⁰⁶ neutrino cross-section divided by neutrino energy and plotted as a function of energy.

¹⁰⁷ **The CP Symmetry Violating Phase Parameter**

¹⁰⁸ The δ parameter showed in the PMNS matrix in equation 1.11 quantifies the charge conju-
¹⁰⁹ gation and parity symmetry violation. The strong and electromagnetic interactions are invariant
¹¹⁰ under CP symmetry, but some weak interaction processes are not. This violating phase param-
¹¹¹ eter is also observed in the quark sector and was already measured. The CP symmetry violating
¹¹² phase parameter is still not observed in the lepton sector.

¹¹³ **The Character of the Neutrino Mass Spectrum (Mass Hierarchy)**

The equation 1.19 limits that the data of neutrino oscillation experiments can only measure the mass-squared differences. Due to the tremendous growth of the neutrino experiment efforts

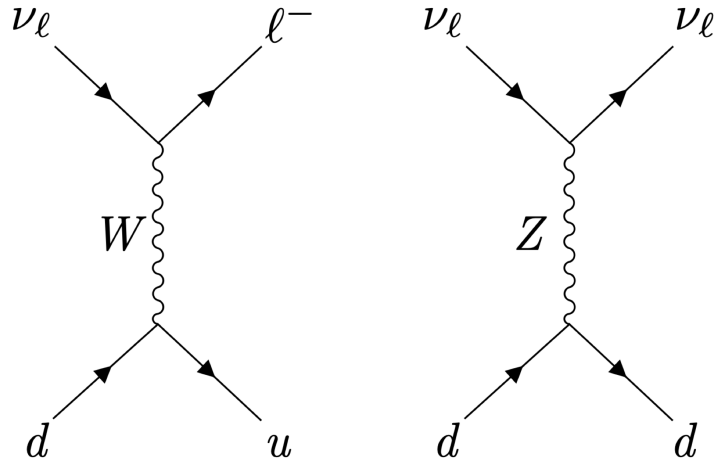


Figure 1.4 | Feynmann Diagrams for the two types of weak interactions

On the left, the Feymman diagram for a Charged Current interaction, carried by a W boson. On the right, the Feymnan diagram for a Neutral Current interaction, carried by a Z boson, [13].

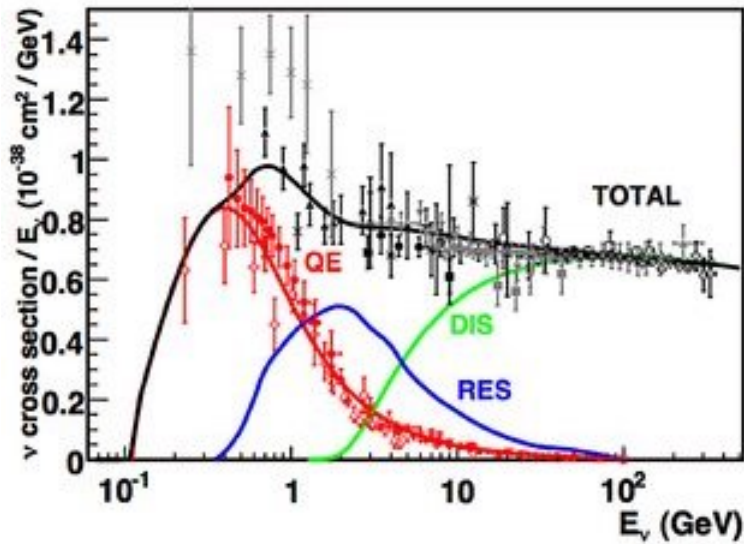


Figure 1.5 | Total CC neutrino cross-section per nucleon as function of energy

Summary of the existing measurements of CC neutrino-nucleon cross-section divided by neutrino energy and plotted as a function of energy. The QE is in red, the resonance in blue, the DIS in green, and the black is the total cross-section, when considering all the previous processes [16].

in the past two decades, it is known that [17]

$$\Delta m_{21}^2 = (7.53 \pm 0.18) \times 10^{-5} \text{ eV}^2 \quad (1.20)$$

and [18]

$$\Delta m_{32}^2 = (2.34 \pm 0.09) \times 10^{-3} \text{ eV}^2 \quad (1.21)$$

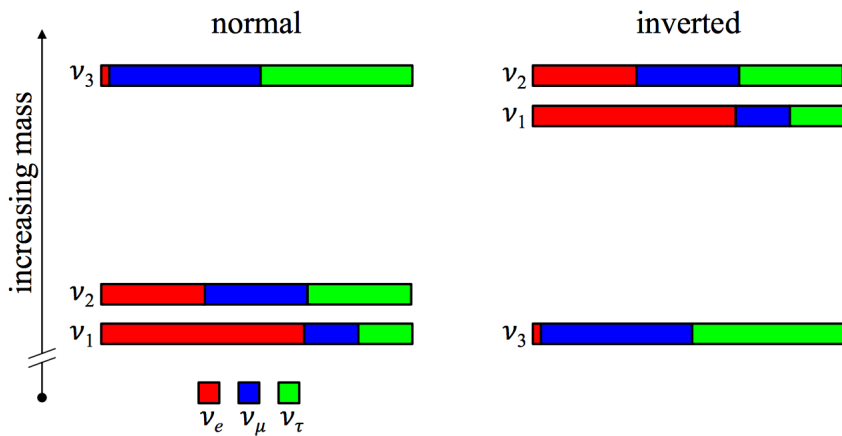


Figure 1.6 | The Mass Hierarchy

The two possible neutrino mass hierarchies. The colors represent the approximate flavor admixtures present in each mass eigenstate [19].

or

$$\Delta m_{32}^2 = (-2.37_{-0.11}^{+0.07}) \times 10^{-3} \text{ eV}^2. \quad (1.22)$$

114 The relative ordering $m_1 < m_2$ is known through observations of solar neutrinos, which are
 115 subject to resonant matter effects in the sun [17]. The value in 1.21 corresponds to what is
 116 called Normal Hierarchy and 1.22 to what is called Inverted Hierarchy. Normal hierarchy is
 117 the condition where the $m_1 < m_2 < m_3$. Inverted hierarchy is the condition where the $m_3 <$
 118 $m_1 < m_2$. A schematic of the normal and inverted hierarchies can be found on figure 1.6. The
 119 precision of neutrino sector measurements has reached a point where the unknown hierarchy is
 120 a major hurdle to further progress [19].

121 The θ_{23} Octant Definition Problem

The θ_{23} parameter is present in both $P_{\nu_\mu \rightarrow \nu_\mu}$ and $P_{\nu_\mu \rightarrow \nu_e}$ calculations. Most of the near past neutrino experiments take advantage of an approximation that considers the existence of only two neutrino flavors due to limitations in their resolution. In this approximation the oscillation probabilities take the form of

$$P_{\nu_\mu \rightarrow \nu_e} \propto \sin^2(2\theta_{23}) \text{ and } P_{\nu_\mu \rightarrow \nu_\mu} \propto \sin^2(2\theta_{23}),$$

122 which implies in a redundancy in the value of θ_{23} , with the possibilities being either $\theta_{23} > \pi/4$
 123 or $\theta_{23} < \pi/4$. In more recent results, experiments such as NuMI Off-axis ν_e Appearance
 124 ($\text{NO}\nu\text{A}$), Main Injector Neutrino Oscillation (MINOS) and Tokai to Kamioka (T2K), do not
 125 use this approximation, resulting in a 2 fold degeneracy solution for the mixing angle θ_{23} . The
 126 latest results were presented by the $\text{NO}\nu\text{A}$ Collaboration and can be seen in figure 1.7, which
 127 shows the two best fit values with their 90% confidence level contours. In this study, $\text{NO}\nu\text{A}$

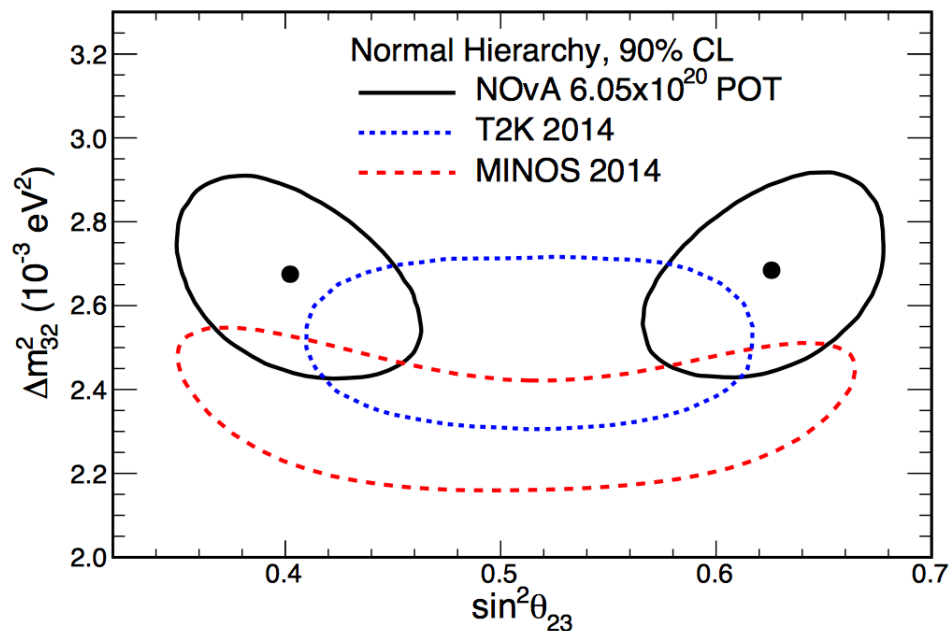


Figure 1.7 | Preliminary θ_{23} results from the NO ν A Experiment

Best fit (black dots) and allowed 90% confidence level regions (solid black curves) of $\sin^2 \theta_{23}$ and Δm_{32}^2 for the normal hierarchy. The dashed curves show MINOS [21] and T2K [22] 90% confidence level contours [20].

128 Collaboration disfavored the maximal mixing ($\sin^2 \theta_{23} = 0.5$) scenario with 2.6σ significance
 129 [20].

130 Low Energy Excess (LEE) Anomalies

131 Over the past few decades, a number of neutrino experiments found inconsistencies between
 132 their expected un-oscillated neutrino flux at low energies and their measurements. Allow me to
 133 describe a few of them briefly. The Liquid Scintillator Neutrino Detector (LSND) at the Los
 134 Alamos Neutron Science Center published a paper in 2001 where they had found an excess
 135 of electron-like antineutrino events in a primarily ν_μ beam [23]. Years later, the MiniBooNE
 136 Experiment probed the same L/E_ν region and also found an excess of electron-like neutrino
 137 and antineutrino events in a primarily ν_μ and $\bar{\nu}_\mu$ respectively, depending of the polarity of the
 138 Booster Neutrino Beam (BNB). Due to limitations on MiniBooNE's detector technology to
 139 separate electron and photon showers, their analysis was inconclusive as to whether the excess
 140 was due to new physics or due to background mis-modeling, [24]. To address this issue, a new
 141 detector with better technology for particle identification was placed near MiniBooNE. This new
 142 experiment, named MicroBooNE, published its results recently, in 2021. In this new report, they
 143 did not find an excess of electron-like neutrino events, but could not refute MiniBooNE's excess
 144 either [25]. The favorite hypothesis for new physics that could explain the LEE phenomena
 145 is that there would exist a fourth neutrino, called sterile neutrino ν_s . This neutrino, unlike

the others, would only interact through the weak force and therefore would only be indirectly observed whenever oscillating from or to one of the other flavors, which would justify the LEE observed, [13]. The LEE Anomaly and the of ν_s s remain open questions in the field.

1.4 LArTPCs in Neutrino Physics

Among a wide variety of detector technologies, Liquid Argon Time Projection Chambers (LArTPCs) present a set of characteristics particularly interesting to neutrino physics. In a more general form, Time Projection Chambers were first proposed by David Nygren, in 1974 [26] and they consist of a volume filled with a sensitive gas or liquid in a strong (~ 500 V/cm) electrical field. When a charged particle passes through the active volume of the detector, the material is ionized, leaving behind a track of ionization charge. This ionization charge is then drifted by the electrical field towards wire planes, where sensitive electronics will record the induction signal, from the passing electrons through the wires, and current, produced by the collection of the electrons by the last set of wires (see figure 1.8). Using a two (or more) plane setup, with at least one being an induction plane and the other being a collection plane, and a light trigger to calculate the drift time of the electrons in the event, it is possible to have a three dimensional calorimetric reconstruction of the track (see figure 1.9).

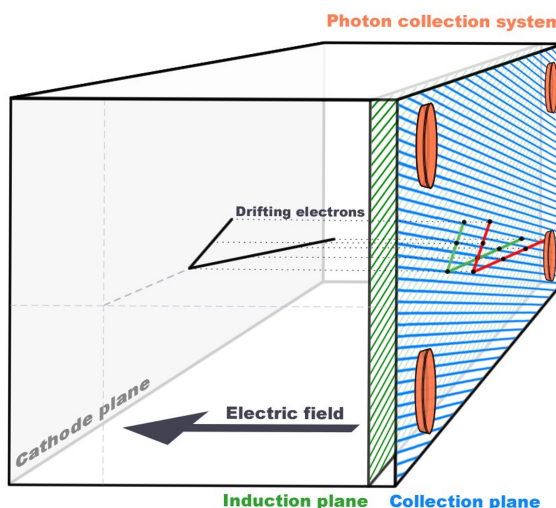


Figure 1.8 | Liquid Argon Time Projection Chamber

Liquid Argon Time Projection Chamber. When a particle passes through its fiducial volume and interacts with the liquid argon, ionization electrons and scintillation light are produced. The electric field drifts the electrons from where they are produced towards the planes of wires (right corner in the figure). Both charge and light produced are read by precision wires and a light collection system (in the figure, the orange bodies behind the wires), respectively.

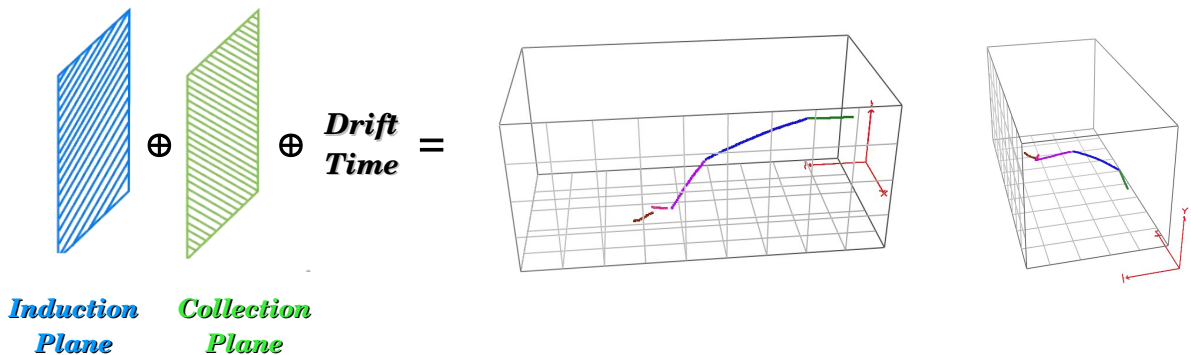


Figure 1.9 | LArTPC read out system

Basic elements of the LArTPC read out system. It is needed a minimum of one induction wire plane, one collection wire plane and a light detection system. The information retrieved by those 3 components allow a 3D track reconstruction [27].

Not long after, in 1977, Carlo Rubia noted that using Liquid Argon (LAr) as active material in a TPC was particularly advantageous for neutrino physics, since:

- it is dense (1.4 g/cm^3), which increases the interaction probability;
- it does not attach electrons, allowing long drift distances, which allows the construction of big detectors;
- it has a high electron mobility;
- argon is the third most abundant gas in the atmosphere, it is easy to obtain and purify, making it relatively cheap;
- it is inert and can be liquified with liquid nitrogen [28]

Ever since, LArTPCs have been the technology of choice of many neutrino physics experiments, such as Imaging Cosmic and Rare Underground Signals (ICARUS), [29], MicroBooNE, [30], Short Baseline Neutrino Detector (SBND), [31], that together form the Short Baseline Neutrino (SBN) Program, and Deep Underground Neutrino Experiment (DUNE) [32], to name a few.

1.5 The Short Baseline Neutrino Program

In a new attempt to get to a conclusion regarding the LEE, described in session, Fermilab created the SBN Program. The program consists of three LArTPCs (SBND, MicroBooNE, and ICARUS) all located along the BNB beam. The principle is that, by having three different detectors of the same technology, exposed to the same beam, and all positioned at a short-baseline range, we will be more accurately be able to constrain our flux of neutrinos and possibly

have an answer to the LEE anomalies observed so far, and search for sterile neutrinos. Beyond that, it aims to study neutrino-nucleus scattering at the GeV energy scale and further develop LArTPC's construction and installation procedures, [33].

Originally, ICARUS was, the first large-scale LArTPC to be used to further our understanding of neutrinos and was located underground at the The Gran Sasso National Laboratory and exposed to the CERN Neutrinos to Gran Sasso (CNGS) beamline [29]. Most recently one of its modules, the T600, was refurbished, upgraded and has its new home at Fermilab, in the BNB beam. ICARUS T600 LArTPC is used as the far detector in the SBN Program. It is a 476ton active mass LArTPC and it seats 600 m from the target.

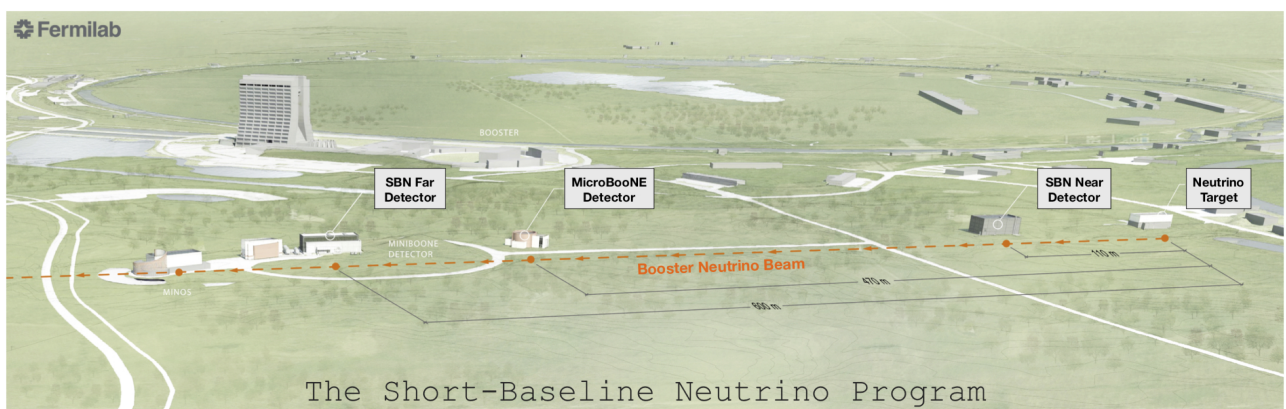


Figure 1.10 | The Short-Baseline Neutrino Program detectors as seen from an upper view at Fermilab. To the right is the neutrino beam target area where 8 GeV protons from the Booster accelerator impinge a beryllium target. The beam is focused along the orange dashed line traveling toward the left (north). The SBND, MicroBooNE, and ICARUS, [33].

The SBND is, as the name implies, the program's near detector and it consists of a 112ton active mass LArTPC is at 110 m from the target. It is currently under installation phase and it is expected to be taking date mid-late next year,2023. In-between ICARUS and SBND, at 470 m from the target, there is MicroBooNE, a 89ton active volume LArTPC that has been taking da since 2015. Where each of the detectors are in the BNB beamline, at Fermilab, is illustrated in figure 1.10. I will later describe in more details SBND and MicroBooNE, as they are the experiments in which I've carried my Ph.D. work.

1.6 The Deep Underground Neutrino Experiment

The Deep Underground Neutrino Experiment (DUNE) is by far the most promising experiment for neutrino physics, as it aims to measure the CP violating phase in the leptonic sector, to determine the character of the neutrino mass spectrum, and to make precision measurements of oscillation parameters. Beyond the neutrino physics goals, DUNE also aims to search for baryon number violating processes and to perform precision measurements of neutrinos from a core-collapse supernova within the Galaxy, if one happens during the experiment's operating

period. To accomplish such bold goals, DUNE counts with a near detector placed at Fermilab and a far detector at the Sanford Underground Research Laboratory in Lead, South Dakota. An intense neutrino beam of up to 2.4 megawatts is produced at Fermilab, crosses the near detector, and travels 1,300 kilometers downstream through Earth's crust to reach the far detector. In figure 1.11 you can see an schematic diagram of the experiment.

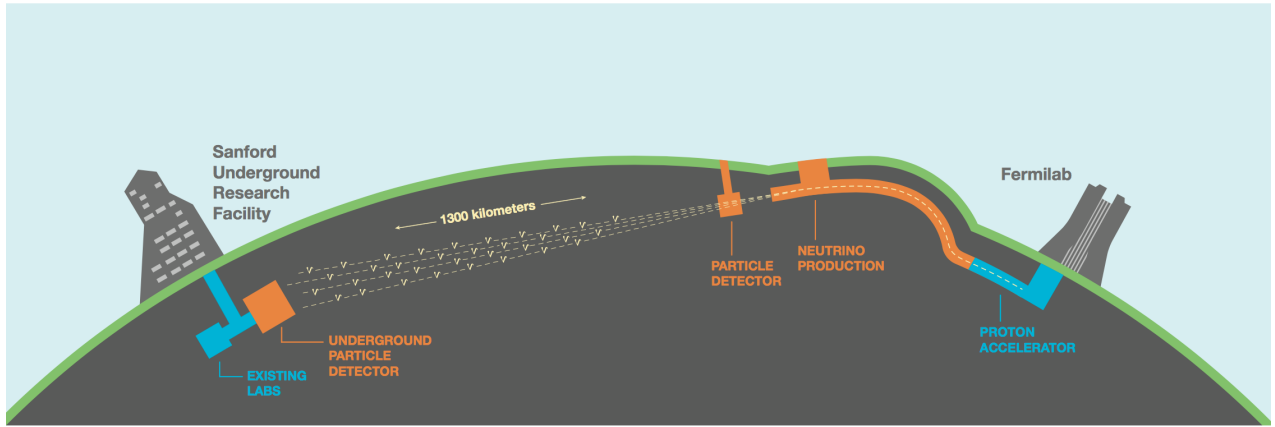


Figure 1.11 | DUNE's full schematic.

The figure shows the full DUNE's schematics, providing a view of the production of the neutrino beam, the Near Detector at Fermilab, the under crust travel of the beam, and the Far Detector at SURF [32].

DUNE's far detector is made of 4 LArTPCs modules, of 10 kton each. The near detector will have a combination of three different detection systems: a modular and optically segmented LArTPC of \approx 300 tons (ND-LAr), a magnetized high-pressure Gas Argon Time Projection Chamber (GArTPC) surrounded by a calorimeter (ND-GAr), a magnetized beam monitor consisting of an electromagnetic calorimeter, an inner target/tracker system and an active LAr target (SAND). [32, 34].

2

216

μ Decay At Rest ν_e -LAr CC Cross Section in MicroBooNE

218

219

220

221 **2.1 Core-Collapse Supernova Neutrino Detection in DUNE**

222 **2.2 μ Decay At Rest (μ DAR)-LAr Physics**

223 **2.3 MicroBooNE**

224 **2.4 NuMI**

225 **2.5 Simulation of μ DAR Events in MicroBooNE**

226 **2.5.1 NuMI Beamline Simulation**

227 **2.5.2 GENIE and MARLEY**

228 **2.6 Reconstruction of μ DAR Events in MicroBooNE**

229 **2.7 Monte Carlo-Data Agreement**

230 **2.8 Background Assessment**

231 **2.9 Data Analysis**

232 **2.10 Conclusion**

3

233

234 **Short Baseline Neutrino Detector's 235 (SBND) Anode Plane Assemblies (APA) 236 Assembly and Installation**

239 **3.1 APA Description**

240 **3.2 APA Quality Assurance (QA) and Quality Control (QC)
241 Tests**

242 **3.3 APA Installation Procedures**

243 **3.4 Status**

4

244

245 Novel LAr Purity Monitor Using Paul 246 Traps

247

248

249 4.1 Purity Monitors for LArTPCs

250 4.1.1 Motivation

251 4.1.2 Current Methods

252 4.2 Paul Trap as a Purity Monitor

253 4.2.1 Concept and Design

254 4.2.2 Simulation

255 Leapfrog integration

256 Paul Trap in Vacuum

257 Paul Trap in Fluid at $T = 0$ K

258 Paul Trap in Fluid at $T \geq 0$ K

259 4.3 Conclusion and Next Steps

Appendix A

260

261

An appendix title

262

263

264 Lorem ipsum dolor sit amet, consectetuer adipiscing elit. Ut purus elit, vestibulum ut, plac-
265 erat ac, adipiscing vitae, felis. Curabitur dictum gravida mauris. Nam arcu libero, nonummy
266 eget, consectetuer id, vulputate a, magna. Donec vehicula augue eu neque. Pellentesque habi-
267 tant morbi tristique senectus et netus et malesuada fames ac turpis egestas. Mauris ut leo. Cras
268 viverra metus rhoncus sem. Nulla et lectus vestibulum urna fringilla ultrices. Phasellus eu tel-
269 lus sit amet tortor gravida placerat. Integer sapien est, iaculis in, pretium quis, viverra ac, nunc.
270 Praesent eget sem vel leo ultrices bibendum. Aenean faucibus. Morbi dolor nulla, malesuada
271 eu, pulvinar at, mollis ac, nulla. Curabitur auctor semper nulla. Donec varius orci eget risus.
272 Duis nibh mi, congue eu, accumsan eleifend, sagittis quis, diam. Duis eget orci sit amet orci
273 dignissim rutrum.

274 Nam dui ligula, fringilla a, euismod sodales, sollicitudin vel, wisi. Morbi auctor lorem non
275 justo. Nam lacus libero, pretium at, lobortis vitae, ultricies et, tellus. Donec aliquet, tortor sed
276 accumsan bibendum, erat ligula aliquet magna, vitae ornare odio metus a mi. Morbi ac orci et
277 nisl hendrerit mollis. Suspendisse ut massa. Cras nec ante. Pellentesque a nulla. Cum sociis
278 natoque penatibus et magnis dis parturient montes, nascetur ridiculus mus. Aliquam tincidunt
279 urna. Nulla ullamcorper vestibulum turpis. Pellentesque cursus luctus mauris.

280 Nulla malesuada porttitor diam. Donec felis erat, congue non, volutpat at, tincidunt tristique,
281 libero. Vivamus viverra fermentum felis. Donec nonummy pellentesque ante. Phasellus adip-
282 iscing semper elit. Proin fermentum massa ac quam. Sed diam turpis, molestie vitae, placerat
283 a, molestie nec, leo. Maecenas lacinia. Nam ipsum ligula, eleifend at, accumsan nec, suscipit a,
284 ipsum. Morbi blandit ligula feugiat magna. Nunc eleifend consequat lorem. Sed lacinia nulla
285 vitae enim. Pellentesque tincidunt purus vel magna. Integer non enim. Praesent euismod nunc
286 eu purus. Donec bibendum quam in tellus. Nullam cursus pulvinar lectus. Donec et mi. Nam
287 vulputate metus eu enim. Vestibulum pellentesque felis eu massa.

288

289

290

Bibliography

- 291 [1] D. Griffiths, **Introduction to Elementary Particle Physics**. Second edition, Wiley-VCH
292 Verlag GmbH & Co. KGaA, Weinheim. ISBN 978-3-527-40601-2. 2008.
- 293 [2] K. V. L. Sarma, **Nobel Leptons**. arXiv:hep-ph/9512420. 1995.
- 294 [3] C. L. Cowan, F. Reines, F. B. Harrison, H. W. Kruse, and A. D. McGuire. **Detection of**
295 **the Free Neutrino: A Confirmation**. Science. 1956.
- 296 [4] E. J. Konopinski, H. M. Mahmoud, **The Universal Fermi Interaction**. Phys. Rev. **92**.
297 1953.
- 298 [5] G. Danby, J-M. Gaillard, K. Goulian, L. M . Lederman, N. Mistry, M. Schwartz, J.
299 Steinberger, **Observation of high-energy neutrino reactions and the existence of two**
300 **kinds of neutrinos**. Phys. Rev. Lett. **9**, 1, 36. 1962.
- 301 [6] G. Rajasekaran, **The Story of the Neutrino**. arXiv:1606.08715. 2016.
- 302 [7] B. Pontecorvo, J. Exptl., **Neutrino Experiments and The Problem of Conservation of**
303 **Leptonic Charge**. Theoret. Phys. **53**, 1717 (1967), Sov. Phys. JETP **26**, 984. 1968.
- 304 [8] S. M. Bilenky, **Neutrino oscillations: brief history and present status**. arXiv:1408.2864.
305 2014.
- 306 [9] K. Kodama *et al.*, **Observation of tau neutrino interactions**. Phys. Lett. B **504**, 218-224.
307 2001.
- 308 [10] Z. Maki *et al.*, **Remarks on the Unified Model of Elementary Particles**. Prog. Theor.
309 Phys. **28**, 870-880. 1962.
- 310 [11] B. Pontecorvo, **Inverse beta processes and nonconservation of lepton charge**. Soviet
311 Phys. JETP. **7**, 172. 1958.
- 312 [12] C. Giunti, C. K. Kim, **Fundamentals of Neutrino Physics and Astrophysics**. Oxford
313 University Press. ISBN 978-0-19-850871-7. 2007.

- 314 [13] L. Yates, **Using the MicroBooNE Liquid Argon Detector to Search for Electron Neu-**
315 **trino Interactions and Understand the MiniBooNE Anomaly.** FERMILAB-THESIS-
316 2022-02. 2022.
- 317 [14] Y. Fukuda *et al.*, **Evidence for oscillation of atmospheric neutrinos.** Phys. Rev. Lett. **81**,
318 1562. 1998.
- 319 [15] Workers doing PMTs checking during Super-Kamiokande's construction. Digital image.
320 Super-Kamiokande collaboration, n.p. Web 17 May, 2010. 16 Jan 2017. [http://www-](http://www-sk.icrr.u-tokyo.ac.jp/sk/gallery/index-e.html)
321 [sk.icrr.u-tokyo.ac.jp/sk/gallery/index-e.html](http://www-sk.icrr.u-tokyo.ac.jp/sk/gallery/index-e.html)
- 322 [16] J. A. Formaggio and G. P. Zeller, **From eV to EeV: Neutrino Cross Sections across**
323 **Energy Scales.** Rev. Mod. Phys. 84, 1307–1341 (2012). arXiv:1305.7513 [hep-ex]
- 324 [17] A. Gando *et al.*, **Neutrino-nucleus quasi-elastic and 2p2h interactions up to 10 GeV.**
325 Phys. Rev. D **88**, 033001. 2013.
- 326 [18] P. Adamson *et al.*, **Combined Analysis of ν_μ Disappearance and $\nu_\mu \rightarrow \nu_e$ Appearance**
327 **in MINOS Using Accelerator and Atmospheric Neutrinos.** Phys. Rev. Lett. **112**,
328 191801 (2014); and update by A. Sousa for MINOS at XXVI International Conference on
329 Neutrino Physics and Astrophysics (Neutrino 2014), proceedings at arXiv:1502.07715.
330 2015.
- 331 [19] R. B. Patterson, **Prospects for measurement of the neutrino mass hierarchy.**
332 arXiv:1506.07917v3. 2016.
- 333 [20] P. Adamson *et al.*, **Measurement of the neutrino mixing angle θ_{23} in NOvA.**
334 arXiv:1701.05891. 2017.
- 335 [21] P. Adamson *et al.*, **Combined Analysis of ν_μ Disappearance and $\nu_\mu \rightarrow \nu_e$ Appearance**
336 **in MINOS Using Accelerator and Atmospheric Neutrinos.** Phys. Rev. Lett. **112**, 191801.
337 2014.
- 338 [22] K. Abe *et al.*, **Measurements of neutrino oscillation in appearance and disappearance**
339 **channels by the T2K experiment with 6.6×10^{20} protons on target.** Phys. Rev. D **91**,
340 072010. 2015.
- 341 [23] A. Aguilar-Arevalo et al. (LSND), **Evidence for neutrino oscillations from the obser-**
342 **vation of ν_e appearance in a ν_μ beam,** Phys. Rev. D 64, 112007 (2001), arXiv:hep-
343 ex/0104049.
- 344 [24] M. Sorel *et al.*, **MiniBooNE: first results on the muon-to-electron neutrino oscillation**
345 **search,** J. Phys.: Conf. Ser. 110 082020, 2008.

- 346 [25] P. Abratenko *et al.*, **Search for an Excess of Electron Neutrino Interactions in Micro-**
347 **BooNE Using Multiple Final State Topologies**. arXiv:2110.14054. 2022.
- 348 [26] D. R. Nygren, **The Time Projection Chamber: A New 4 pi Detector for Charged**
349 **Particles**. eConf, vol. C740805, p. 58, 1974.
- 350 [27] R. Acciarri (LArIAT Collaboration), **LArIAT: Liquid Argon In a Testbeam Internal**
351 **report**. DocDB-1975
- 352 [28] C. Rubbia, **The Liquid Argon Time Projection Chamber: A New Concept for Neu-**
353 **trino Detectors**. 1977.
- 354 [29] S. Amerio *et al.*, (ICARUS Collaboration), **Design, construction and tests of the**
355 **ICARUS T600 detector**. Nucl. Instr. and Meth. in Phys. Res. A **527**, 329. 2004.
- 356 [30] H. Chen *et al.*, **A Proposal for a New Experiment Using the Booster and NuMI Neu-**
357 **trino Beamlines: MicroBooNE**. 2007.
- 358 [31] **Short-Baseline Near Detector (SBND)**. n.d. Retrieved from <http://sbn-nd.fnal.gov>
- 359 [32] A. Abed Abud *et al.*, **Snowmass Neutrino Frontier: DUNE Physics Summary: Execu-**
360 **tive Summary of DUNE Physics Program**. arXiv:2203.06100. 2022
- 361 [33] P. Machado, O. Palamara, and D. Schmitz, **The Short-Baseline Neutrino Program at**
362 **Fermilab**. arXiv:1903.04608. 2019.
- 363 [34] Matteo Vicenzi, for the DUNE collaboration, **SAND - System for on-Axis Neutrino De-**
364 **tection - in the DUNE Near Detector complex**. The 22nd International Workshop on
365 Neutrinos from Accelerators (NuFact2021). Italy, 2021.